Spectrochimica Acta Part A: Molecular and Biomolecular Spectroscopy 171 (2017) 168–173

Contents lists available at ScienceDirect

Spectrochimica Acta Part A: Molecular and Biomolecular Spectroscopy

journal homepage: www.elsevier.com/locate/saa

Aptamer biosensor for *Salmonella typhimurium* detection based on luminescence energy transfer from Mn^{2+}-doped $NaYF_4$:Yb, Tm upconverting nanoparticles to gold nanorods

Keyi Cheng, Jianguo Zhang, Liping Zhang, Lun Wang *, Hongqi Chen *

Anhui Key Laboratory of Chemo-Biosensing, Key Laboratory of Functional Molecular Solids, Ministry of Education, College of Chemistry and Materials Science, Anhui Normal University, Wuhu 241000, PR China

ARTICLE INFO

Article history:
Received 6 April 2016
Received in revised form 26 July 2016
Accepted 8 August 2016
Available online 09 August 2016

Keywords:
Luminescence energy transfer
Upconverting nanoparticles
Gold nanorods
Salmonella typhimurium

ABSTRACT

A highly sensitive luminescent bioassay for the detection of *Salmonella typhimurium* was fabricated using Mn^{2+}-doped $NaYF_4$:Yb,Tm upconversion nanoparticles (UCNPs) as the donor and gold nanorods (Au NRs) as the acceptor and utilizing an energy transfer (LET) system. Mn^{2+}-doped $NaYF_4$:Yb,Tm UCNPs with a strong emission peak at 807 nm were obtained by changing the doped ion ratio. Carboxyl-terminated Mn^{2+}-doped $NaYF_4$:Yb,Tm UCNPs were coupled with *S. typhimurium* aptamers, which were employed to capture and concentrate *S. typhimurium*. The electrostatic interactions shorten the distance between the negatively charged donor and the positively charged acceptor, which results in luminescence quenching. The added *S. typhimurium* leads to the restoration of luminescence due to the formation of UCNPs-aptamers-*S. typhimurium*, which repels the UCNPs-aptamers from the Au NRs. The LET system does not occur because of the nonexistence of the luminescence emission band of Mn^{2+}-doped $NaYF_4$:Yb,Tm UCNPs, which had large spectral overlap with the absorption band of Au NRs. Under optimal conditions, the linear range of detecting *S. typhimurium* was 12 to 5×10^5 cfu/mL ($R = 0.99$). The limit of detection for *S. typhimurium* was as low as 11 cfu/mL in an aqueous buffer. The measurement of *S. typhimurium* in milk samples was satisfied in accordance with the plate-counting method, suggesting that the proposed method was of practical value in the application of food security.

1. Introduction

At present, conventional meat and dairy producer contaminations and food poisoning caused by *Salmonella* have become serious issues of food safety that jeopardize human health [1]. With the problem of growing food safety concerns, there is a need to establish simple, efficient, rapid, and sensitive detection methods for *Salmonella* [2]. The methods for detecting *Salmonella* include traditional detection methods, immunological methods [3] and polymerase chain reaction (PCR) [4], However, although the traditional detection method results are accurate and reliable, the cycle is long, complicated to operate, and unable to meet the rapid detection needs. The reagents of the immunological method are costly and prone to false positive signals. Although the PCR sensitivity is good, the method in the extraction of nucleic acid samples is susceptible to pollution. PCR conditions requiring multiple groups for the desired result can be achieved, and the different bases can-not be discriminated between conspecific strains of different serotypes due to the length of the PCR, so the specificity is poor.

Rare-earth-doped upconversion nanoparticles (UCNPs) are capable of emitting strong visible fluorescence excited by low power continuous wavelength lasers as the excitation source (typically 980 nm) [5]. UCNPs have shown outstanding luminescent properties as fluorescent biolabels over the traditional organic fluorophores [6]. The signal-to-background ratio can be greatly improved because of the low toxicity, narrow emission peaks, high resistance to photobleaching, large Stokes shifts, low autofluorescence background [7] and high chemical stability [8,9]. Furthermore, to achieve high photoluminescence efficiency, Mn^{2+}-doped $NaYF_4$:Yb,Tm UCNPs have been prepared by a hydrothermal method [10]. In addition, the carboxyl-functionalized UCNPs serve as the luminescence donor. Gold nanorods (Au NRs) have several advantages, such as good biocompatibility, low toxicity and no photo-induced damage or light interference [11]. These properties point to the strong potential of gold nanorods in the LET system for use as acceptors for NIR range bioassays.

Aptamers, which have high affinity and specificity, are single-stranded DNA or RNA sequence fragments, that can be obtained through a vitro systematic evolution of ligands by exponential enrichment (SELET) [12]. Aptamers bind to target molecules with similar affinity and specificity as antibodies [13], and they provide a variety of advantages over antibodies because of their chemical stability [14],

* Corresponding authors.
E-mail addresses: wanglun@mail.ahnu.edu.cn (L. Wang), hq80chen@mail.ahnu.edu.cn (H. Chen).

http://dx.doi.org/10.1016/j.saa.2016.08.012
1386-1425/

ease of synthesis and modification [15,16], inexpensiveness and minimal immunogenicity [17,18]. Based on these advantages [19], aptamers have been designed as electrochemical [20], fluorescent [21] and colorimetric [22] sensors for a wide range of targets [23].

Herein, we describe the design of a turn-on luminescence energy transfer system, in which Mn^{2+}-doped $NaYF_4$:Yb,Tm UCNPs immobilized aptamers onto the surface as the energy donor and Au NRs acted as the energy acceptor. The electrostatic interactions shorten the distance between the negatively charged donor and the positively charged acceptor, which results in luminescence quenching [24]. The added *S. typhimurium* leads to restoration of luminescence due to the formation of UCNPs-aptamer-*S. typhimurium*, which keeps the UCNPs-aptamer away from the Au NRs. This method has a low detection limit and good selectivity, and can detect its targeted bacteria in a short time. The method may promote the application of UCNPs in food safety analysis, especially for the detection of pathogenic bacteria, toxins and viruses.

2. Experimental

2.1. Chemicals and materials

$MnCl_2 \cdot 4H_2O$, $HAuCl_4 \cdot 3H_2O$, $AgNO_3$, $NaBH_4$, and thulium nitrate (99.95%) were purchased from Aladdin Reagent Corporation (Shanghai, China). Ytterbium (III) chloride hexahydrate and yttrium nitrate hexahydrate were purchased from Jinan Henghua Science and Technology Co. Ltd. (China). Poly(acrylic acid) (PAA), 4-(2-hydroxyethyl)-1-piperazi-neethanesulfonic acid (HEPES), 2-(N-morpholino) ethanesulfonic acid (MES), 1-Ethyl-3-(3-dimethylaminopropyl) carbodiimide hydrochloride (EDC·HCl), diethylene glycol (DEG) (99 + %), *N*-hydroxysuccinimide (NHS), and cetyltrimethyl ammonium bromide (CTAB) were obtained from Sigma-Aldrich (U.S.A.). Sodium citrate, toluene, ethanol, NaF and concentrated hydrochloric acid were purchased from Sinopharm Chemical Reagent Co. (China). *S. typhimurium* aptamers were synthesized by and ascorbic acid was acquired from Shanghai Sangon Biological Science and Technology Company (Shanghai, China). The sequence of the *S. typhimurium* aptamer was 5′-NH_2-GCA ATG GTA CGG TAC TTC CTC GGC ACG TTC TCA GTA GCG CTC GCT GGT CAT CCC ACA GCT ACG TCA AAA GTG CAC GCT ACT TTG CTA A-3′. The strains of *S. typhimurium* were obtained from Wuhu Institute for Food and Drug Control (China). All of the reagents were analytical grade and were used without any further purification. All solutions were prepared with ultrapure water.

2.2. Instruments and characterizations

Transmission electron microscopy (TEM) was performed using a JEOL model 2010 HR instrument operating at 200 kV accelerating voltage to investigate the size and morphology of nanomaterials. The crystal structure was analyzed with a Rigaku RU-200b X-ray powder diffractometer (XRD) with nickel-filtered Cu Kα radiation (λ = 0.14518 nm) 20° ≤ 2θ ≤ 80°. Upconversion nanoparticle fluorescence spectra were measured on a Hitachi F-4600 fluorescence spectrophotometer, which was attached to an external 980 nm laser (Beijing Hi-Tech Optoelectronic Co., China) instead of an internal excitation source. Ultraviolet–visible (UV–vis) absorption spectra were recorded using a Hitachi UV–4100 spectrophotometer. The zeta potential was measured using a Malvern Zetasizer nano ZS90 apparatus (Malvern Instruments, Malvern, United Kingdom).

2.3. Procedures

2.3.1. Synthesis and surface modification of Mn^{2+}-doped $NaYF_4$:Yb^{3+}, Tm^{3+} UCNPs

Mn^{2+}-doped $NaYF_4$:Yb^{3+}, Tm^{3+} UCNPs were prepared according to our previously reported procedure with minor alteration [25]. Briefly, $Y(NO_3)_3$ (0.2 M, 1.2 mL), $MnCl_2 \cdot 4H_2O$ (1.2 M, 145 μL), $YbCl_3$ (0.1 M, 1 mL), $Tm(NO_3)_3$ (0.1 M, 100 μL), and sodium citrate (0.1 M, 1.75 mL) were mixed with ultrapure water (2.1 mL) in a beaker. Then, ethanol (15 mL) and CTAB (0.1 g) were added under magnetic stirring to form a homogeneous solution. Subsequently, aqueous NaF (1.0 M, 6 mL) was added dropwise. The mixed solution was stirred for 2 h. Concentrated nitric acid (1 mL) was added to obtain the complex precursor solution. The solution was transferred into a 50 mL Teflon-lined autoclave and treated at 180 °C for 4 h. The system was allowed to cool to room-temperature naturally. The products were deposited at the bottom of the vessel, were collected by centrifugation at 10,000 rpm for 5 min, and washed once with anhydrous ethanol and three times with deionized water.

Surface modification of Mn^{2+}-doped $NaYF_4$:Yb^{3+}, Tm^{3+} UCNPs was completed using a ligand exchange method [26]. A mixture of PAA (0.2 g) and DEG (16 mL) was added to a four-necked flask and was vigorously stirred under a protective nitrogen flow, and the flask was heated to 110 °C. In quick succession, a toluene solution containing the Mn^{2+}-doped $NaYF_4$:Yb^{3+}, Tm^{3+} UCNPs (16 mg in 2 mL) was quickly injected into the flask. The system was heated to 150 °C and was maintained for 1.5 h. Then, the resulting solution was naturally cooled to room temperature, and hydrochloric acid (0.1 M, 2 mL) was added. The final products were obtained via centrifugation (10,000 rpm, 10 min) and were washed several times with deionized water.

2.3.2. Preparation of amino aptamer-upconversion nanoparticle conjugates

The procedure for the preparation of oligonucleotide-conjugated UCNPs was adapted from a previously reported method [27]. In brief, 1.6 mg of carboxyl-modified UCNPs was first dissolved in 2 mL of 10 mM MES buffer solution at pH 5.6, and sulfo-NHS (1.1 mg) and

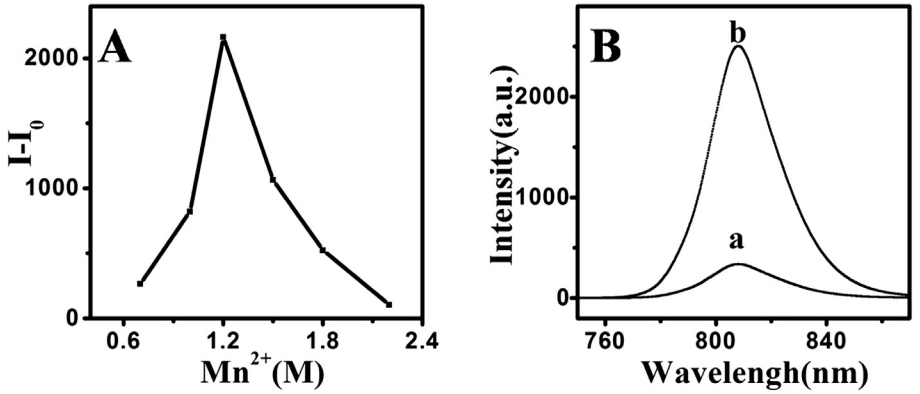

Fig. 1. (A) The effect of added Mn^{2+} on the luminescence intensity of the Mn^{2+}-doped $NaYF_4$:Yb,Tm UCNPs. (B) Emission spectra of (a) the $NaYF_4$:Yb,Tm UCNPs and (b)the $NaYF_4$:Yb,Tm UCNPs with 1.2 M of $MnCl_2 \cdot 4H_2O$.

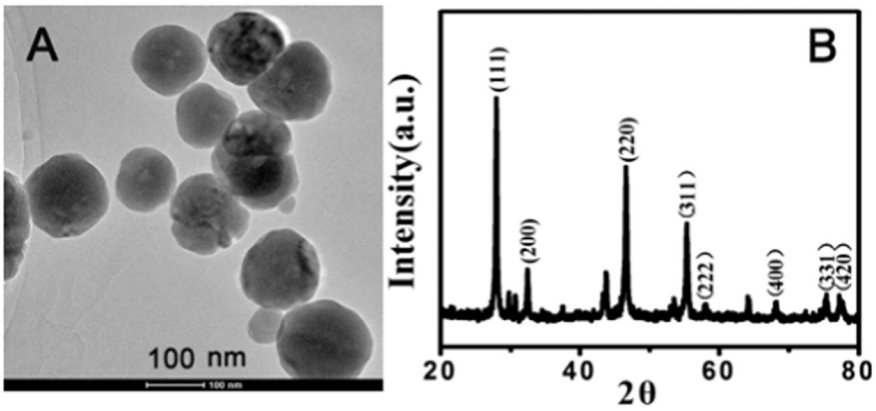

Fig. 2. TEM image (A) and XRD pattern (B) of Mn^{2+}-doped $NaYF_4$:Yb^{3+}, Tm^{3+} UCNPs.

EDC (0.5 mg) were introduced into the mixture. After shaking gently for 2 h at 30 °C, the UCNPs were separated by centrifugation and were washed twice with ultrapure water. The activated PAA-UCNPs were dissolved in 2 mL of 10 mM HEPES buffer solution at pH 7.2. Then, 48 μL of 12.5 μM amino-modified aptamer was added. The mixture was incubated at 30 °C in a reciprocating oscillator for another 4 h. The amino groups on the 5′ end of the aptamer were covalently attached to the carboxyl groups on the UNPs surface through a catalyzed condensation reaction. The final products were collected by twice centrifugation, were washed with ultrapure water after removal of the supernatant and were redispersed in fresh Tris-HCl buffer (10 mM Tris-HCl, pH 7.4, 1 mM $MgCl_2$, 140 mM NaCl, 5 mM KCl).

2.3.3. Synthesis of gold nanorods

The GNRs were synthesized by a slightly modified version of the seed-mediated growth procedure in CTAB surfactant solution [28,29,30].

Seeds. CTAB solution (0.2 M, 5 mL) was mixed with $HAuCl_4$ (5.0×10^{-4} M, 5 mL) solution. To this stirred solution, ice-cold $NaBH_4$ solution (10 mM, 0.6 mL) was added. The resulting seed solution immediately turned brownish-yellow and was vigorously stirred for 2 min before storing at 25 °C.

Growth solutions. A gold growth solution was prepared by adding $HAuCl_4$ (1 mM, 5 mL) to CTAB (0.2 M, 5 mL). $AgNO_3$ (4 mM, 0.25 mL) and ascorbic acid (78.8 mM, 70 μL) were gradually added until the solution turned colorless. The final addition was the seeds (12 μL), aged for approximately 40 min, The solution was kept in a 28 °C water bath for the GNRs to go to completion. The products were collected by centrifugation at 10,000 rpm for 10 min and were washed several times with ultrapure water. All glassware was cleaned with aqua regia and dried in an oven.

2.3.4. Procedures for S. typhimurium determination

In a typical test, carboxyl-functionalized Mn^{2+}-doped $NaYF_4$:Yb^{3+}, Tm^{3+} UCNPs (32 μg/mL) were mixed with GNRs (3 pM) in Tris-HCl buffer (10 mM Tris-HCl, pH 7.4, 1 mM $MgCl_2$, 140 mM NaCl, 5 mM KCl). Subsequently, various concentrations ($12.0–5.0 \times 10^4$ cfu/mL) of *S. typhimurium* were added to this mixture and further incubated at 30 °C for 40 min. The fluorescence was assayed using an F-4600 fluorescence spectrophotometer, which was equipped with a 980 nm laser as the excitation light. All experiments were repeated three times.

3. Results and discussion

3.1. Characteristics of the Mn^{2+}-doped $NaYF_4$:Yb, Tm UCNPs and GNRs

During the process to synthesize the Mn^{2+}-doped $NaYF_4$:Yb,Tm UCNPs, we determined the quantity of $MnCl_2 \cdot 4H_2O$ that needed to optimize the optical properties. When the $MnCl_2 \cdot 4H_2O$ concentration was 1.2 M, the luminescence intensity reached a maximum (Fig. 1). The TEM image of the nanocrystals in Fig. 2 (A) showed that the as-synthesized UCNPs were spherical in shape with a uniform size. In this work, $NaYF_4$:Yb^{3+}, Tm^{3+} UCNPs were synthesized via a hydrothermal technique, and remarkably enhanced upconversion luminescence was achieved by Mn^{2+} doping. The structure of the resultant UCNPs samples was characterized by X-ray powder diffraction (XRD), as shown in Fig. 2

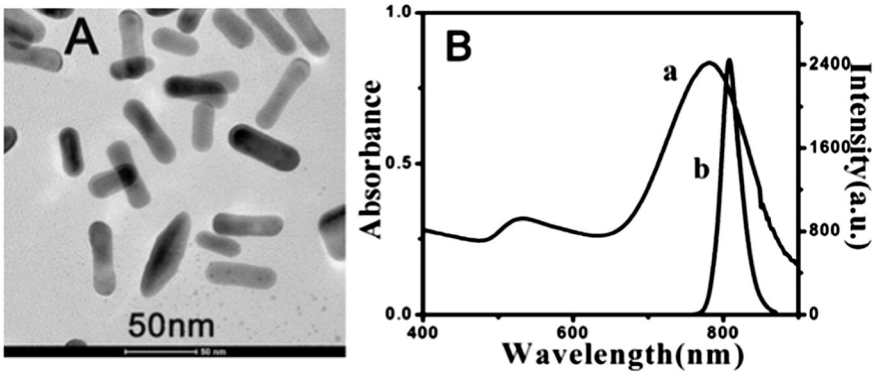

Fig. 3. (A) TEM image of Au NRs. (B) Spectral overlap: (a) SPR absorption spectrum of Au NRs and (b) the upconversion spectrum of Mn^{2+}-doped $NaYF_4$:Yb^{3+}, Tm^{3+} UCNPs.

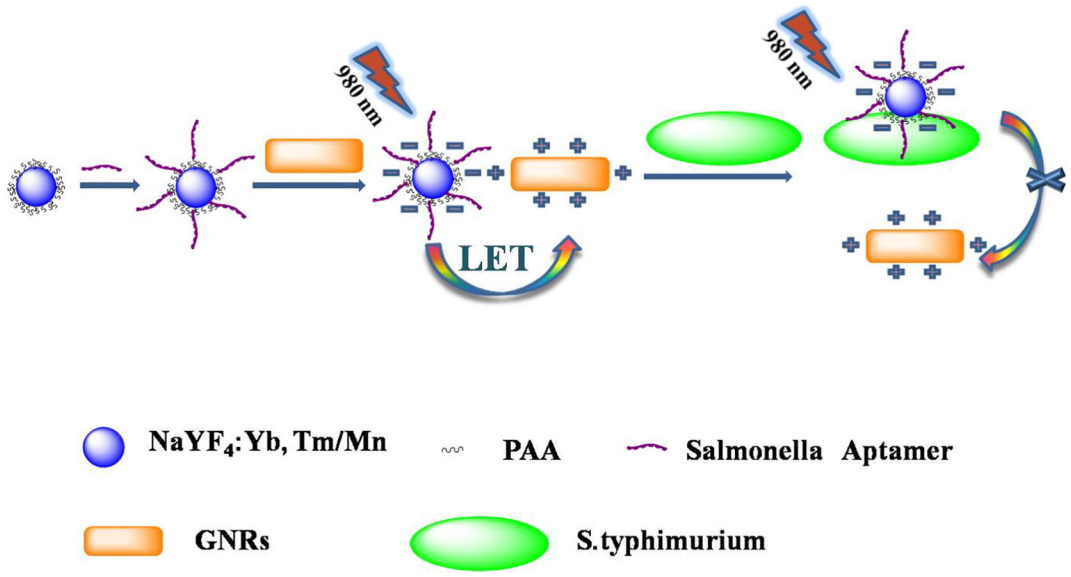

Fig. 4. Schematic illustration of the fabrication process of biofunctionalized nanoparticles and principle of the performed bioassay.

(B), which revealed that the diffraction peaks could be indexed to the standard JCPDS 6-0342 cubic α-$NaYF_4$. To build the UCNPs-based LET biosensor, PAA was used to form a carboxyl-terminated surface through a ligand-exchange approach, eventually making the UCNPs highly water dispersible [31]. The resultant carboxyl-functionalized UCNPs can be attached to the amino aptamer. To prove the surface modification and biological link of the UCNPs successfully, zeta potential experiments was conducted and indicated that the PAA-modified UCNPs were negatively charged(−27.4 mV) [32].

Fig. 3 (A) displays the TEM image of the Au NRs. The absorbance spectra of the Au NRs were successfully collected, resulting in two resonance absorption bands at 530 nm and 780 nm (Fig. 3 (B), a), which presented large overlaps with the emission band of the Mn^{2+}-doped $NaYF_4$:Yb^{3+}, Tm^{3+} UCNPs (Fig. 3 (B), b), a condition that was employed to create a new near-infrared (NIR) biological detection system.

3.2. Principle of determining S. typhimurium levels

The carboxyl-functionalized upconverting nanoparticles were conjugated with the aptamers and acted as the donor (negatively charged).

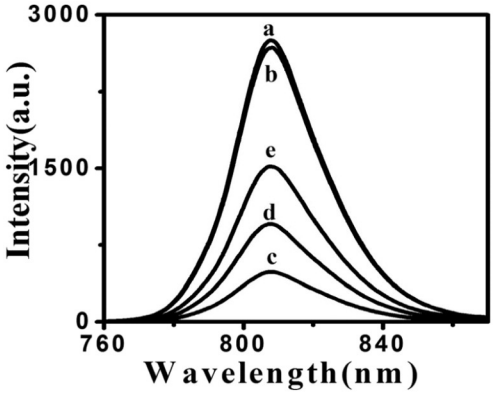

Fig. 5. Luminescence emission spectra of UCNPs-aptamer under different conditions: (a) UCNPs-aptamer; (b) UCNPs-aptamer + target (1.25×10^4 cfu/mL); (c) UCNPs-aptamer + Au NRs; (d) UCNPs-aptamer + Au NRs + target (125 cfu/mL); (e) UCNPs-aptamer + Au NRs + target (1.25×10^4 cfu/mL). UCNPs-aptamer concentration: 32 μg/mL. Au NRs concentration: 3 pM. Experiments were performed in Tris-HCl buffer (10 mM Tris-HCl, pH 7.4, 1 mM $MgCl_2$, 140 mM NaCl, 5 mM KCl).

Au NRs served as the acceptor (positively charged). On the basis of the electrostatic interactions, the donor and the acceptor were brought into close proximity, which resulted in luminescence quenching. Subsequently, *S. typhimurium* was added to the system. The binding affinity between *S. typhimurium* and the complementary aptamers was stronger than the electrostatic interactions. This procedure is illustrated in Fig. 4.

3.3. Control experiments

The occurrence of LET and the detection for *S. typhimurium* using turn-on luminescence after the recognition of its aptamer was demonstrated in Fig. 5. As shown in this figure, the fluorescence spectrum of the UCNPs-aptamer without Au NRs exhibited strong fluorescence emission at 807 nm (a). No obvious changes were observed for the fluorescence intensity when *S. typhimurium* was added (b). However, in the presence of Au NRs, >80% of the UCNPs fluorescence was quenched, which was attributed to the energy transfer from the UCNPs to Au NRs (c). Meanwhile, upon addition of the target, there was a significant luminescence intensity recovery (d and e).

3.4. Optimization of the reaction conditions

In this experiment, to further obtain sensitive detection, the assay conditions, such as UCNPs-aptamer concentration, Au NRs concentration, were investigated by fluorescence spectra.

Fig. 6A displays the influence of different concentrations of UCNPs-aptamer on the response of *S. typhimurium*. The experimental results showed that the response of *S. typhimurium* reached the maximum when the concentration of the UCNPs-aptamer was 32 μg/mL. Fig. 6B shows the fluorescence quenching of the UCNPs-aptamer at different concentrations of Au NRs, the luminescence intensity decreased substantially upon the addition of 3 pM Au NRs. Hence, 3 pM Au NRs was used in the following experiments.

3.5. Target detection

Determination of *S. typhimurium* was performed in Tris-HCl buffer under optimal conditions. Fig. 7A shows that the luminescence was dramatically recovered with the addition of increasing amounts of *S. typhimurium* to the system. Fig. 7B shows the linear relationship

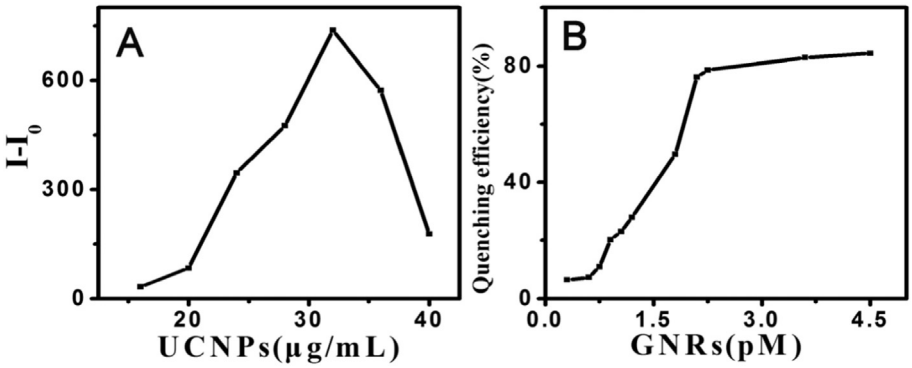

Fig. 6. (A) Luminescence intensity: various concentrations of UCNPs-aptamer + Au NRs (3 pM) + *S. typhimurium* (2.5×10^3 cfu/mL). (B) Luminescence quenching efficiency: UCNPs-aptamer (32 μg/mL) + various concentration of Au NRs. Experiments were performed in Tris-HCl buffer (10 mM Tris-HCl, pH 7.4, 1 mM $MgCl_2$, 140 mM NaCl, 5 mM KCl).

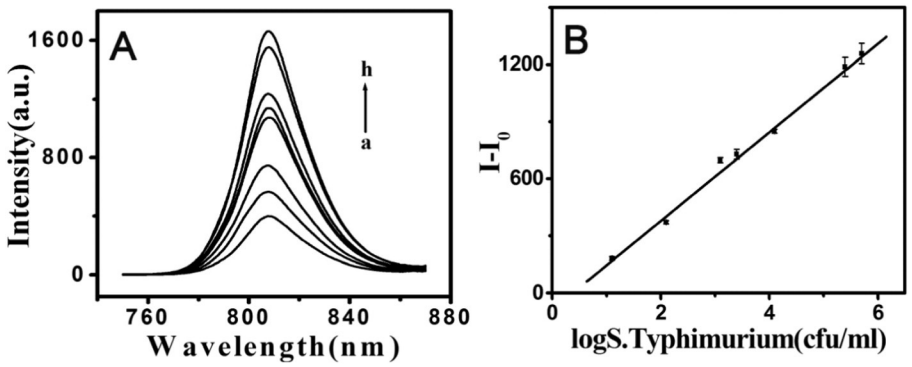

Fig. 7. (A) The luminescence spectra of the UCNPs-aptamer with different concentrations of *S. typhimurium*: a → h: 0, 12, 125, 1250, 2500, 1.25×10^4, 2.5×10^5, and 5×10^5 cfu/mL. (B) The linear relationship between the luminescence recovery and the concentration of *S. typhimurium* within the range of 12 to 5×10^5 cfu/mL Conditions: GNRs: 3 pM; Mn^{2+}-doped $NaYF_4$:Yb,Tm UCNPs: 32 μg/mL, Experiments were performed in Tris-HCl buffer (10 mM Tris-HCl, pH 7.4, 1 mM $MgCl_2$, 140 mM NaCl, 5 mM KCl).

between the logarithm of the *S. typhimurium* concentration and the increased luminescence intensity ($\Delta I = I - I_0$), in which I_0 and I represent the intensity of luminescence of the LET system in the absence and presence, respectively, of *S. typhimurium* at different amounts. The range of detection of *S. typhimurium* was linear from 12 to 5×10^5 cfu/mL with a correlation coefficient (R) of 0.99, and the LOD of the proposed method was calculated as 11 cfu/mL according to the 3σ criterion, in which σ represents the standard deviation of the blank (n = 10).

3.6. Specificity

For the selectivity assay, parallel experiments were performed to test the detection selectivity. The fluorescence signal changes induced by the binding of two other pathogenic bacteria, such as *E. coli* and *S. aureus*, were investigated under the same experimental conditions ($1 \times 10^{4.5}$ cfu/mL). *E. coli* and *S. aureus* did not exhibit obvious fluorescence increases in the signal, whereas $1 \times 10^{3.5}$ cfu/mL *S. typhimurium* resulted in fluorescence restoration (Fig. 8). The results demonstrated that the high specificity of the proposed method depends on the intrinsic properties of the aptamer, which can serve as a specific ligand for *S. typhimurium*. The response induced by non-specific binding was negligible.

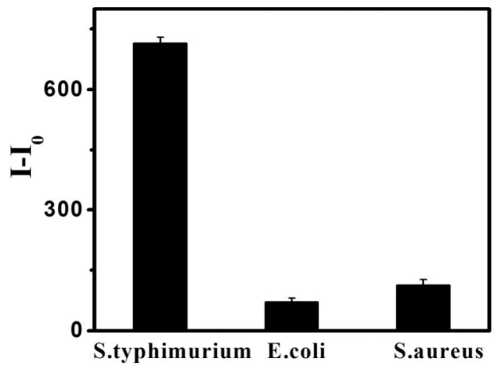

Fig. 8. The response signal changes in the upconversion luminescence for *S. typhimurium*, *E. coli* and *S. aureus*. Error bars indicate the standard deviation (n = 3).

3.7. Application to milk samples

To test the accuracy of the applied bioanalysis method for real sample detection, milk was selected as the sample and was pre-treated as follows: 5 mL of milk sample was collected by centrifugation at 7000 rpm for 10 min at 10 °C, the upper layer of cream was removed, and diluted with deionized water in a 1:20 ratio before filtering with a disposable syringe filter. The analysis results are given in Table 1. There was no significant difference in the results obtained using this proposed method and the plate counting method. The above results indicated the proposed method has potential for quantitative *S. typhimurium* detection in real samples.

Table 1
Comparison of the results obtained for *S. typhimurium* in the spiked milk.

Sample	Spiked concentration (cfu/mL)	Measured concentration (cfu/mL)	Recovery (%)
1	10^3	$(0.857 \pm 0.179) \times 10^3$	85.7%
2	10^4	$(1.055 \pm 0.375) \times 10^4$	105.5%
3	10^5	$(1.015 \pm 0.302) \times 10^5$	101.5%

4. Conclusions

A turn-on LET system based on upconversion nanoparticles as the donor coupled with gold nanorods as the acceptor was successfully developed and evaluated for the simple, rapid and specific detection of *S. typhimurium*. Compared to other materials, UCNPs have its intrinsic advantages, such as high quantum yields and sharp emission lines. More importantly, the background fluorescence from biomolecules contained in solution can be entirely eliminated through the use of infrared 980 nm laser excitation, which can provide high sensitivity. The Au NRs, with a longitudinal SPR band at 780 nm as the acceptor, improve the efficiency. In addition, the aptamers are stable and highly specific to the target bacteria, demonstrating the potential to detect other bacteria by substituting suitable aptamers [33,34,35]. In conclusion, the present biosensing method has the potential to detect various types of coexisting pathogenic bacteria for food safety control.

Acknowledgements

This work was financially supported by Natural Science Foundation of China (21275008, 21475001), Anhui Provincial Natural Science Foundation (1408085QB40), Foundation for Innovation Team of Bioanalytical Chemistry and Special and Excellent Research Fund of Anhui Normal University.

References

[1] Z. Sahar, A. Desouky, E. Ehab, M. Marwa, J. Appl. Sci. Environ. Manag. 13 (2009) 83–92.
[2] P.Y. Cheung, K.M. Kam, Food Res. Int. 45 (2012) 802–808.
[3] P. Preechakasedkit, K. Pinwattana, W. Dungchai, W. Siangproh, W. Chaicumpa, P. Tongtawe, O. Chailapakul, Biosens. Bioelectron. 31 (2012) 562–566.
[4] D. Wiemer, U. Loderstaedt, H. von Wulffen, S. Priesnitz, M. Fischer, E. Tannich, R.M. Hagen, Int. J. Med. Microbiol. 301 (2011) 577–584.
[5] C. Li, J. Lin, J. Mater. Chem. 20 (2010) 6831.
[6] R. Deng, X. Xie, M. Vendrell, Y. Chang, X. Liu, J. Am. Chem.Soc. 133 (2011) 20168–20171.
[7] H.S. Mader, O.S. Wolfbeis, Anal. Chem. 82 (2010) 5002–5004.
[8] W. Zheng, P. Huang, D. Tu, E. Ma, H. Zhu, X. Chen, Chem. Soc. Rev. 44 (2015) 1379–1415.
[9] K. Gagandeep, Y. Dwivedi, A. Rai, S.B. Rai, Spectrochim. Acta Part A 95 (2012) 511–516.
[10] J. Zhang, S. Wang, N. Gao, D. Feng, L. Wang, H. Chen, Biosens. Bioelectron. 72 (2015) 282–287.
[11] L. Tong, Y. Zhao, T.B. Huff, M.N. Hansen, A. Wei, J.X. Cheng, Adv. Mater. 19 (2007) 3136–3141.
[12] D.A. Daniels, H. Chen, B.J. Hicke, K.M. Swiderek, L. Gold, P. Natl. Acad. Sci. 100 (2003) 15416–15421.
[13] A. Bini, M. Minunni, S. Tombelli, S. Centi, M. Mascini, Anal. Chem. 79 (2007) 3016–3019.
[14] J. Zheng, G.F. Cheng, P.G. He, Y.Z. Fang, Talanta 80 (2010) 1868–1872.
[15] Y. Wang, L. Bao, Z. Liu, D.W. Pang, Anal. Chem. 83 (2011) 8130–8137.
[16] S. Tombelli, M. Minunni, M. Mascini, Biosens. Bioelectron. 20 (2005) 2424–2434.
[17] H. Xing, N.Y. Wong, Y. Xiang, Y. Lu, Curr. Opin. Chem. Biol. 16 (2012) 429–435.
[18] H. Xing, K. Hwang, J. Li, S.F. Torabi, Y. Lu, Curr. Opin. Chem. Eng. 4 (2014) 79–87.
[19] L. Yang, X. Zhang, M. Ye, J. Jiang, R. Yang, T. Fu, Y. Chen, K. Wang, C. Liu, W. Tan, Adv. Drug Deliv. Rev. 63 (2011) 1361–1370.
[20] J. Zhang, S. Song, L. Wang, D. Pan, C. Fan, Nat. Protoc. 2 (2007) 2888–2895.
[21] B. Li, H. Wei, S. Dong, Chem. Commun. 1 (2006) 73–75.
[22] W.H. Wu, J. Zhang, M.Q. Zheng, Y.H. Zhong, J. Yang, Y.H. Zhao, W.P. Wu, W. Ye, J. Wen, Q. Wang, J.X. Lu, PLoS One 7.11 (2012) e48999.
[23] S.F. Torabi, Y. Lu, Curr. Opin. Biotechnol. 28 (2014) 88–95.
[24] H. Chen, Y. Guan, S. Wang, Y. Ji, M. Gong, L. Wang, Langmuir 30 (2014) 13085–13091.
[25] F. Yuan, H. Chen, J. Xu, Y. Zhang, Y. Wu, L. Wang, Chem-Eur. J. 20 (2014) 2888–2894.
[26] C. Liu, Z. Wang, X. Wang, Z. Li, SCIENCE CHINA Chem. 54 (2011) 1292–1297.
[27] H. Chen, F. Yuan, S. Wang, J. Xu, Y. Zhang, L. Wang, Biosens. Bioelectron. 48 (2013) 19–25.
[28] B. Nikoobakht, M.A. El-Sayed, Chem. Mater. 15 (2003) 1957–1962.
[29] C.J. Murphy, L.B. Thompson, D.J. Chernak, J.A. Yang, S.T. Sivapalan, S.P. Boulos, J. Huang, A.M. Alkilany, P.N. Sisco, Curr. Opin. Colloid. In. 16 (2011) 128–134.
[30] X.C. Jiang, M.P. Pileni, Colloid. Surf. A-Physicochem. Eng. Asp. 295 (2007) 228–232.
[31] L. Wang, Y. Zhang, Y. Zhu, Nano Res. 3 (2010) 317–325.
[32] S. Wu, N. Duan, Z. Shi, C. Fang, Z. Wang, Talanta 128 (2014) 327–336.
[33] N. Duan, S. Wu, C. Zhu, X. Ma, Z. Wang, Y. Yu, Y. Jiang, Anal. Chim. Acta 723 (2012) 1–6.
[34] S. Wu, N. Duan, Z. Shi, C. Fang, Z. Wang, Anal. Chem. 86 (2014) 3100–3107.
[35] E. Torres-Chavolla, E.C. Alocilja, Biosens. Bioelectron. 24 (2009) 3175–3182.